APPLIED PHYSICS LETTERS 109, 221111 (2016)

Heterogeneously integrated III–V-on-silicon 2.3x μm distributed feedback lasers based on a type-II active region

Ruijun Wang,[1,2,a)] Stephan Sprengel,[3] Aditya Malik,[1,2] Anton Vasiliev,[1,2] Gerhard Boehm,[3] Roel Baets,[1,2] Markus-Christian Amann,[3] and Gunther Roelkens[1,2]

[1]*Photonics Research Group, Ghent University-imec, Technologiepark-Zwijnaarde 15, B-9052 Ghent, Belgium*
[2]*Center for Nano- and Biophotonics (NB-Photonics), Ghent University, B-9052 Ghent, Belgium*
[3]*Walter Schottky Institut, Technische Universität München, Am Coulombwall 4, 85748 Garching, Germany*

(Received 12 October 2016; accepted 19 November 2016; published online 2 December 2016)

We report on 2.3x μm wavelength InP-based type-II distributed feedback (DFB) lasers heterogeneously integrated on a silicon photonics integrated circuit. In the devices, a III–V epitaxial layer stack with a "W"-shaped InGaAs/GaAsSb multi-quantum-well active region is adhesively bonded to the first-order silicon DFB gratings. Single mode laser emission coupled to a single mode silicon waveguide with a side mode suppression ratio of 40 dB is obtained. In continuous-wave regime, the 2.32 μm laser operates close to room temperature (above 15 °C) and emits more than 1 mW output power with a threshold current density of 1.8 kA/cm^2 at 5 °C. A tunable diode laser absorption measurement of CO is demonstrated using this source. *Published by AIP Publishing.*
[http://dx.doi.org/10.1063/1.4971350]

Silicon photonics beyond the telecommunication wavelength range attracts interest as it is a promising platform to build compact photonics system for the integrated spectroscopic sensors.[1,2] In the 2–3 μm wavelength range, many important gases exhibit narrow and dense absorption lines.[3] Therefore, a number of silicon photonics components have been developed in this wavelength range for spectroscopic gas sensing applications, such as low-loss waveguides, high performance arrayed waveguide grating (AWG) spectrometers and photodetectors.[4–6] In order to realize compact silicon photonics gas sensor systems, the on-chip single mode lasers are required. Such single mode silicon photonics laser sources operating at telecommunication wavelengths have been demonstrated over the last years[7–9] but are to be demonstrated in the 2–3 μm wavelength range. Recently, a heterogeneously integrated Fabry-Perot laser on silicon at 2 μm wavelength was demonstrated based on molecular bonding technology and strained InGaAs type-I heterostructures.[10] But the emission wavelength of the strained InGaAs type-I material system is limited to around 2.3 μm.[11] GaSb-based type-I heterostructures can be used to realize light sources operated in 2–3 μm wavelength range.[12–14] However, the heterogeneous processes of GaSb-based material are not as well-established as InP-based material, resulting in low process yield and poor device performance.[1] In the recent years, InP-based type-II quantum well lasers with emission wavelengths up to 2.7 μm were reported.[15,16] The lasing wavelength in this material system can possibly be extended to longer wavelengths as photoluminescence up to 3.9 μm wavelength has been demonstrated.[17] These results indicate that compact III–V/silicon photonics sensor systems can be realized by integrating InP-based type-II active structures with silicon. Recently, we demonstrated heterogeneously integrated InP-based type-II Fabry-Perot lasers on silicon photonics integrated circuits (PICs) based on adhesive bonding technology.[18] However, for many spectroscopic sensing applications, a single mode laser is essential.

In this paper, we report heterogeneously integrated single mode lasers on a silicon PIC at wavelengths beyond 2 μm, based on an InP-based type-II active region and a distributed feedback (DFB) laser geometry. The III–V layer stack is adhesively bonded to the silicon waveguide circuit using a divinylsiloxane-bis-benzocyclobutene (DVS-BCB) bonding layer. The laser can produce more than 1 mW of single mode output at a wavelength of 2.32 μm with a threshold current density of 1.8 kA/cm^2 at 5 °C, and lases continuous wave (CW) up to 17 °C. A side mode suppression ratio (SMSR) better than 40 dB is obtained. The emission wavelength can be tuned with laser temperature and injection current. The demonstration of tunable diode laser absorption spectroscopy (TDLAS) of CO using such a silicon photonics laser is also presented.

The heterogeneously integrated InP-based type-II DFB laser consists of a III–V gain section in the center, on top of a silicon distributed feedback grating, and III–V/silicon spot size converters (SSCs) on both sides, as schematically shown in Fig. 1. The III–V epitaxial layer stack consists of a 200 nm thick *n*-InP contact layer, an active region surrounded by a 130 nm thick GaAsSb and 250 nm thick AlGaAsSb separate confinement heterostructures (SCH) layer, a 1.5 μm thick *p*-InP cladding and a 100 nm p^+-InGaAs contact layer. The active region contain six periods of a "W"-shaped quantum well structure, each separated by a 9 nm thick $GaAs_{0.58}Sb_{0.42}$ layer. Every "W"-shaped quantum well structure consists of two 2.6 nm InGaAs layers and one 2.9 nm GaAsSb layer. Detailed information about the design of the InP-based type-II epitaxial layer stack can be found in Ref. 18.

In the gain section, the optical mode is strongly confined in the III–V waveguide, resulting in a high modal gain. A 5 μm wide and a 1000 μm long III–V mesa is used here. The 5 μm waveguide width is chosen to achieve low waveguide propagation loss and high optical confinement in the active

a)Electronic mail: ruijun.wang@intec.ugent.be.

Reuse of AIP Publishing content is subject to the terms at: https://publishing.aip.org/authors/rights-and-permissions. Download to IP: 157.193.240.1 On: Fri, 02 Dec 2016 14:22:46

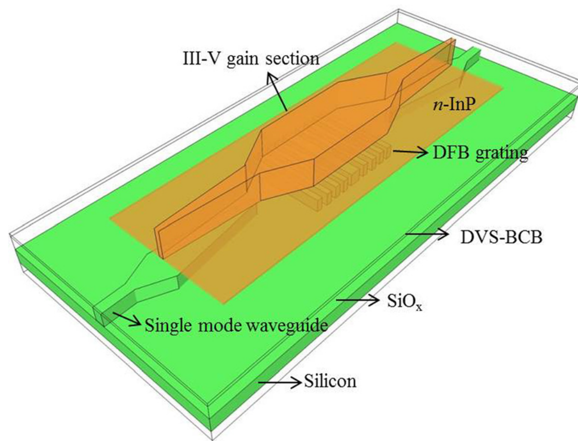

FIG. 1. Three-dimensional schematic view of the heterogeneously integrated DFB laser.

region. When the BCB bonding layer thickness is 60 nm, the calculated confinement factor of the TE polarized fundamental mode in the quantum wells is 10.1%. The first-order DFB gratings with an etch depth of 180 nm in a 400 nm silicon device layer are defined beneath the gain section. The tail of the optical mode interacts with this grating, which sets the emission wavelength of the laser. A quarter-wave shifted grating structure is implemented to break modal degeneracy and ensure single mode lasing. In this paper, two DFB lasers with a grating pitch of 348 nm and 353 nm are studied. Both have a grating duty cycle of 50%. The coupling coefficient κ is calculated to be 62 cm^{-1}. The light is coupled from the III–V active region to the silicon waveguide using the III–V/silicon SSCs by tapering both the III–V and silicon waveguides. The SSC has two tapered sections, as described in detail in Ref. 18. In the first section, the III–V waveguide quickly tapers from 5 μm to 1.2 μm over a length of 50 μm. In the second section, the III–V waveguide tapers down to 0.5 μm, while the silicon waveguide underneath tapers from 0.2 μm to 3 μm over a length of 180 μm. Simulations indicate that the coupling efficiency of the III–V/silicon SSC is higher than 90% when the III–V taper tip is narrower than 500 nm.

The silicon PICs are fabricated in imec's CMOS pilot line on 200 mm silicon-on-insulator (SOI) wafers with a 400 nm thick silicon device layer and a 2 μm thick buried oxide layer. The silicon structures are patterned by a 193 nm deep UV lithography, followed by a 180 nm deep dry etch in the 400 nm thick silicon layer to define silicon rib waveguide and gratings. Then, SiO_2 is deposited and planarized by a chemical mechanical polishing process down to the silicon waveguide. The III–V epitaxial layer stack is adhesively bonded onto the processed silicon PIC wafer using a 60 nm thick DVS-BCB layer.[19] Afterward, the InP substrate is removed by HCl wet etching, using an InGaAs etch stop layer to leave the laser epitaxial structure attached to the SOI waveguide circuits. Then, the DFB lasers are processed in the III–V membrane. SiN_x is used as a hard mask to define the III–V waveguide. A key process to realize high-performance DFB lasers based on this structure is the definition of the III–V taper tip. In order to realize very narrow taper tips using a 320 nm UV contact lithography, an anisotropic HCl wet etching of the *p*-InP layer is carried out. This anisotropic etching can create a "V"-shaped mesa, as shown in Fig. 2(a), which reduces the lithographic pattern size requirement for the taper tip formation. With a 1 μm wide taper tip pattern defined in the SiN_x hard mask, the bottom width of the *p*-InP after HCl etching can be reduced to less than 200 nm. The active region is etched by using a 1:1:20:70 H_3PO_4:H_2O_2:citric acid:H_2O solution. After the III–V mesa processing, the devices are passivated by DVS-BCB. The Ni/Ge/Au and Ti/Au layers are deposited as *n*-contact and *p*-contact, respectively. The general DFB laser process flow is the same as that used to fabricate our previously demonstrated photodetectors,[6] enabling the co-integration of both types of devices on the same silicon PIC. A scanning electron microscopy (SEM) image of the longitudinal cross-section of the fabricated laser is shown in Fig. 2(b), showing the quarter wave shifted silicon DFB grating, the DVS-BCB bonding layer and the III–V p-i-n layer stack.

The fabricated DFB lasers are characterized by collecting the light coupled to the silicon waveguides through the integrated fiber-to-chip grating couplers. Standard single mode fiber (SMF-28) is used for light collection, which is connected to an optical spectrum analyzer (OSA, Yokogawa AQ6375). The coupling efficiency of the grating coupler is measured on reference structures and used to determine the laser power in the silicon waveguides. At 2.35 μm, the measured fiber-to-chip coupling efficiency is around -10 dB, and the 3 dB bandwidth is 150 nm. Figures 3(a) and 3(b) show the light-current-voltage (L-I-V) curve of the DFB with the 348 nm (Laser1) and 353 nm (Laser2) period first-order gratings, respectively. The series resistance of the lasers is around 8 Ω. In order to characterize the L-I properties of the lasers, both

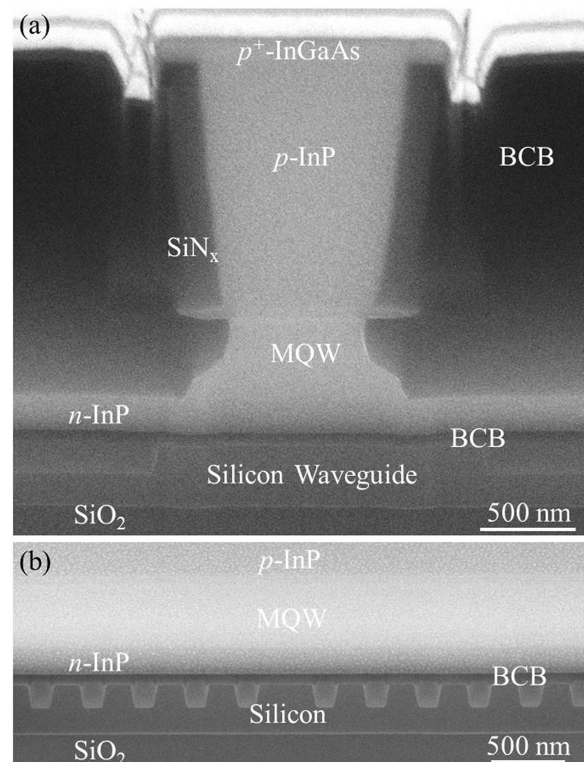

FIG. 2. SEM image of the device: (a) cross section of the III–V/silicon spot size converter and (b) longitudinal cross section of the III–V-on-silicon laser structure.

Reuse of AIP Publishing content is subject to the terms at: https://publishing.aip.org/authors/rights-and-permissions. Download to IP: 157.193.240.1 On: Fri, 02 Dec 2016 14:22:46

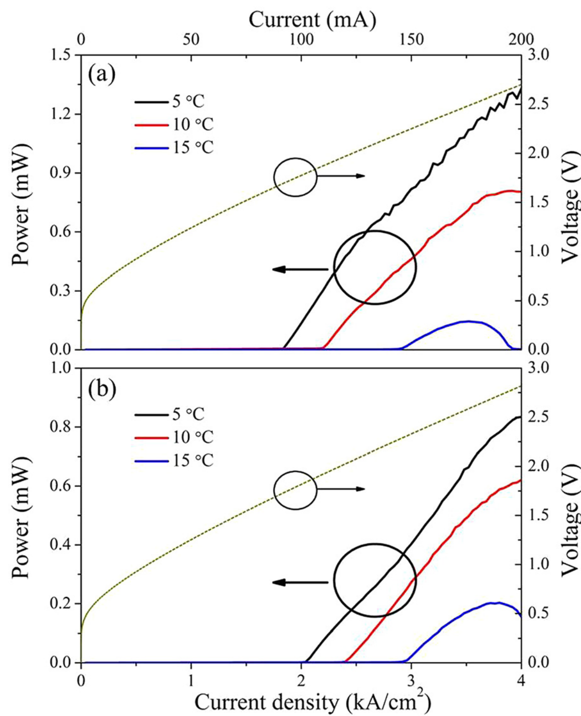

FIG. 3. L-I-V curve of the DFB laser with a 348 nm (a) and 353 nm (b) period first-order grating, measured in continuous wave.

devices are measured in a CW regime at the temperatures of 5 °C, 10 °C and 15 °C. At 5 °C, Laser1 and Laser2 have a threshold current of 90 mA (corresponding to a current density of 1.8 kA/cm^2) and 102 mA (2.04 kA/cm^2), respectively, which is much lower than the first demonstrated "W"-shaped InGaAs/GaAsSb quantum well lasers grown on InP substrate (∼3.2 kA/cm^2 at 0 °C).[15] The maximum on-chip output power is around 1.3 mW and 0.8 mW for Laser1 and Laser2, respectively. The lower threshold current and higher output power of Laser1 can be attributed to the gain at the lasing wavelength of Laser1 being higher than that of Laser2 at 5 °C. As the temperature increases, the gain spectrum shifts to longer wavelength, which results in an output power of Laser2 being higher than that of Laser1 at 15 °C. The maximum CW operating temperature of the two lasers is around 17 °C. The threshold current and operating temperature can be improved by reducing the thermal resistance of the devices, e.g., by further reducing the DVS-BCB thickness and connecting the top *p*-contact to the silicon substrate. Reducing the series resistance by optimizing the metallization processes also can further improve the device performance.

The laser emission spectra are acquired using a Yokogawa AQ6375 OSA with a resolution bandwidth of 0.1 nm. Figure 4 shows the high resolution output spectra of Laser1 and Laser2, both biased at 190 mA at a temperature of 10 °C. As the DFB grating pitch increases from 348 nm to 353 nm, the lasing wavelength shifts from 2320 nm to 2350 nm. This provides a method to realize a 2 μm range DFB laser array by adjusting the grating pitch of the silicon grating structure. Such a DFB laser array can be used to monitor several gases using a single III–V epitaxial layer stack. Single mode lasing with an SMSR around 40 dB is obtained, which can be improved to >43 dB at 5 °C. From the emission spectra of Laser1 and Laser2, a stop band of

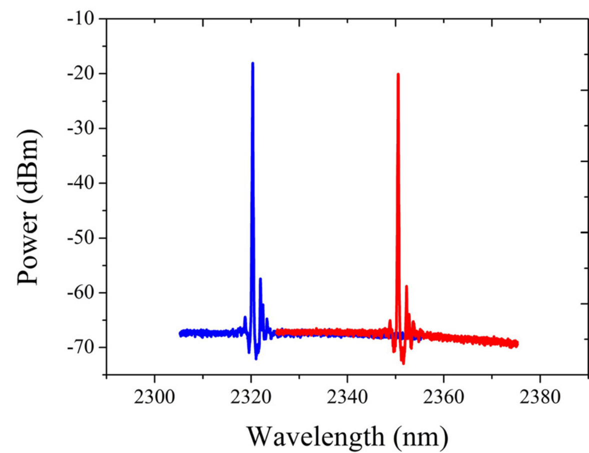

FIG. 4. Emission spectra of DFB lasers with different grating period (348 nm and 353 nm), measured at 10 °C and with 190 mA bias current.

3.2 nm wide is deduced. According to the coupled-mode theory of DFB lasers,[20] the normalized coupling coefficient κL is calculated to be 5.5 for the 1000 μm long laser structure.

Figures 5(a) and 5(b) show the evolution of the laser emission spectra as a function of the heat-sink temperature at a fixed injected current of 190 mA for DFB Laser1 and Laser2, respectively. The dependence of the lasing wavelength on temperature is plotted in the insets. The measured temperature-tuning rate is ∼0.15 nm/°C. This tuning rate is determined by the change in effective index of the DFB lasers. The laser emission spectra for different bias currents at a heat-sink temperature of 10 °C are shown in Figs. 5(c) and 5(d). The corresponding laser wavelengths versus bias currents for heat-sink temperatures of 5 °C, 10 °C and 15 °C are shown in the two insets. The current-tuning rate is about 0.01 nm/mA for both lasers. Single-mode lasing behavior is observed over the whole bias current range, as the heat-sink temperature varies from 5 °C to 15 °C. This indicates that no substantial spatial hole burning occurs in the two DFB lasers at high bias currents. At heat-sink temperature of 10 °C, an SMSR better than 35 dB over injection current of 120 mA–210 mA is obtained.

As the first step on the path to TDLAS on a silicon PIC, the direct absorption spectroscopy of CO in a gas cell is carried out using our heterogeneously integrated DFB lasers as the light source. The gas cell contains pure CO at pressure of 740 Torr, with a length of 10 cm and is AR-coated for 2.34 μm wavelength. In the sensing setup, the gas cell is positioned between the DFB laser with the grating period of 348 nm and the detector. The light is coupled from the DFB laser to a single mode fiber through the on-chip grating coupler and then coupled into and out of the gas cell through a collimator. The laser heat-sink temperature is fixed at 13 °C during the measurement. As the injection current increases, the DFB laser emission shifts to longer wavelength. When the lasing wavelength reaches the CO absorption wavelength, a strong dip can be observed in the L-I curve. Using the current-wavelength relationship extracted from measured data at 13 °C, the TDLAS spectrum of CO is shown in Fig. 6. The current sweep step is 0.5 mA, which corresponds to a wavelength step of around 5 pm. It can be found that the peak absorption intensity and fitted full width at half maximum

Reuse of AIP Publishing content is subject to the terms at: https://publishing.aip.org/authors/rights-and-permissions. Download to IP: 157.193.240.1 On: Fri, 02 Dec 2016 14:22:46

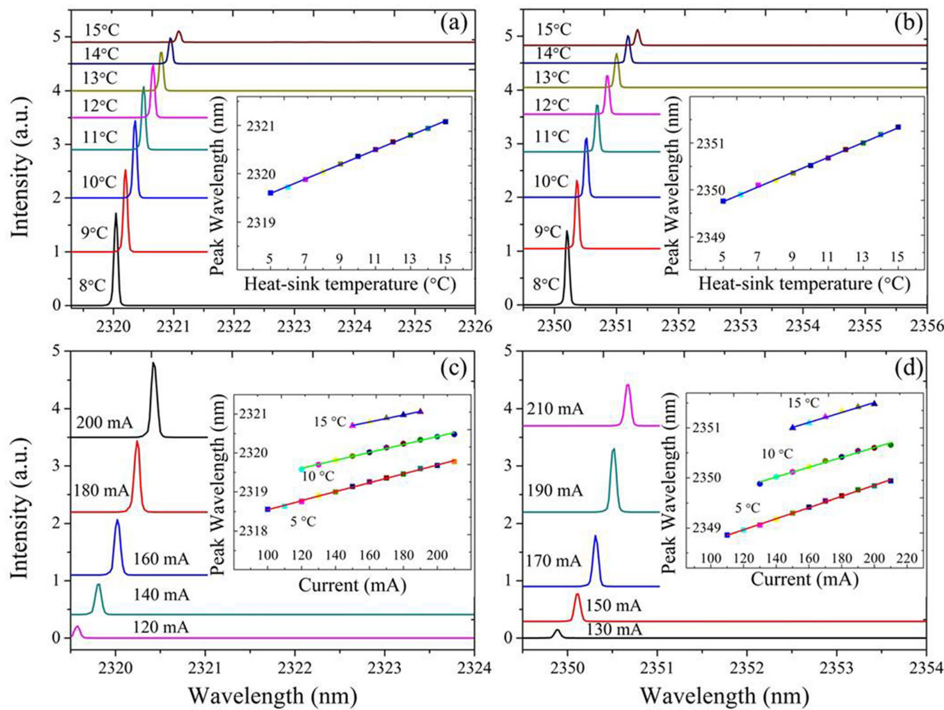

FIG. 5. Evolution of the lasing spectra as a function of the heat-sink temperature for the laser with grating period of 348 nm (a) and 353 nm (b), with both devices biased at 190 mA. The inset pictures show the dependence of the lasing wavelength on temperature; (c) and (d): Emission wavelength as a function of bias current for the two lasers operated at a heat-sink temperature of 10 °C. The inset pictures show the laser wavelength as a function of injected current at the temperatures of 5 °C, 10 °C and 15 °C.

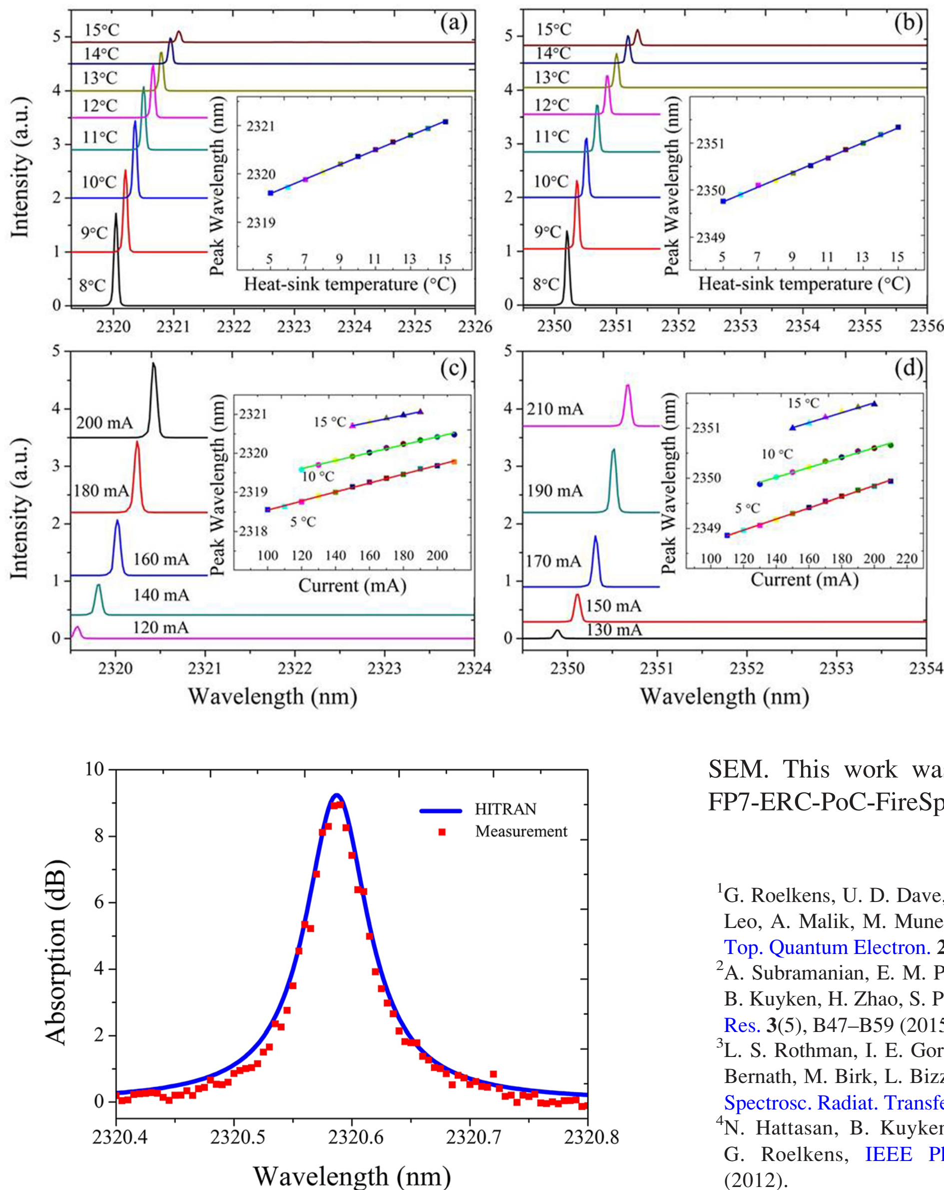

FIG. 6. TDLAS spectrum of CO and the corresponding HITRAN spectrum.

(FWHM) of the experimental TDLAS spectrum match very well to the reference HITRAN values.[3] These results showcase the potential of this laser source for on-chip spectroscopic gas sensing.

We have demonstrated the heterogeneous 2.3x μm wavelength DFB lasers integrated on a silicon PIC. In the lasers, an InP-based type-II epitaxial structure with "W"-shaped InGaAs/GaAsSb quantum wells is bonded to a silicon waveguide circuit, comprising the distributed feedback structure. Single-mode emission with SMSR of 40 dB is obtained. At 2.32 μm wavelength, the laser has a maximum laser output of 1.3 mW and a threshold current density of 1.8 kA/cm^2 at 5 °C. The lasers exhibit a temperature tuning rate around 0.15 nm/°C and a current tuning rate of 0.01 nm/°C. A direct absorption measurement of CO indicates that such silicon photonic sources are suitable for gas sensing.

The authors would like to thank S. Verstuyft and M. Muneeb for processing help and L. Van Landschoot for SEM. This work was supported by FP7-ERC-MIRACLE, FP7-ERC-PoC-FireSpec and FP7-ERC-InSpectra.

[1]G. Roelkens, U. D. Dave, A. Gassenq, N. Hattasan, C. Hu, B. Kuyken, F. Leo, A. Malik, M. Muneeb, and E. M. P. Ryckeboer *et al.*, IEEE J. Sel. Top. Quantum Electron. **20**(4), 394–404 (2014).
[2]A. Subramanian, E. M. P. Ryckeboer, A. Dhakal, F. Peyskens, A. Malik, B. Kuyken, H. Zhao, S. Pathak, A. Ruocco, A. De Groote *et al.*, Photonics Res. **3**(5), B47–B59 (2015).
[3]L. S. Rothman, I. E. Gordon, Y. Babikov, A. Barbe, D. C. Benner, P. F. Bernath, M. Birk, L. Bizzocchi, V. Boudon, L. R. Brown *et al.*, J. Quant. Spectrosc. Radiat. Transfer **130**, 4–50 (2013).
[4]N. Hattasan, B. Kuyken, F. Leo, E. Ryckeboer, D. Vermeulen, and G. Roelkens, IEEE Photonics Technol. Lett. **24**(17), 1536–1538 (2012).
[5]R. Wang, M. Muneeb, S. Sprengel, G. Boehm, A. Malik, R. Baets, M.-C. Amann, and G. Roelkens, Opt. Express **24**(8), 8480–8490 (2016).
[6]R. Wang, S. Sprengel, M. Muneeb, G. Boehm, R. Baets, M. C. Amann, and G. Roelkens, Opt. Express **23**(20), 26834–26841 (2015).
[7]A. W. Fang, E. Lively, Y.-H. Kuo, D. Liang, and J. E. Bowers, Opt. Express **16**(7), 4413–4419 (2008).
[8]S. Keyvaninia, S. Verstuyft, L. Van Landschoot, F. Lelarge, G.-H. Duan, S. Messaoudene, J. M. Fedeli, T. De Vries, B. Smalbrugge, E. J. Geluk *et al.*, Opt. Lett. **38**(24), 5434–5437 (2013).
[9]Z. Wang, B. Tian, M. Pantouvaki, W. Guo, P. Absil, J. V. Campenhout, C. Merckling, and D. V. Thourhout, Nat. Photonics **9**, 837 (2015).
[10]A. Spott, M. Davenport, J. Peters, J. Bovington, M. J. R. Heck, E. J. Stanton, I. Vurgaftman, J. Meyer, and J. Bowers, Opt. Lett. **40**(7), 1480–1483 (2015).
[11]G. Boehm, M. Grau, O. Dier, K. Windhorn, E. Roenneberg, J. Rosskopf, R. Shau, R. Meyer, M. Ortsiefer, and M. C. Amann, J. Cryst. Growth **301–302**, 941–944 (2007).
[12]S. Forouhar, R. M. Briggs, C. Frez, K. J. Franz, and A. Ksendzov, Appl. Phys. Lett. **100**(3), 031107 (2012).
[13]Q. Gaimard, L. Cerutti, R. Teissier, and A. Vicet, Appl. Phys. Lett. **104**(16), 161111 (2014).
[14]T. Lehnhardt, M. Hümmer, K. Rößner, M. Müller, S. Höfling, and A. Forchel, Appl. Phys. Lett. **92**(18), 183508 (2008).
[15]S. Sprengel, A. Andrejew, K. Vizbaras, T. Gruendl, K. Geiger, G. Boehm, C. Grasse, and M.-C. Amann, Appl. Phys. Lett. **100**(4), 041109 (2012).
[16]S. Sprengel, G. Veerabathran, A. Andrejew, A. Köninger, G. Boehm, C. Grasse, and M. C. Amann, Proc. SPIE **9382**, 93820U (2015).

Reuse of AIP Publishing content is subject to the terms at: https://publishing.aip.org/authors/rights-and-permissions. Download to IP: 157.193.240.1 On: Fri, 02 Dec 2016 14:22:46

[17]S. Sprengel, C. Grasse, P. Wiecha, A. Andrejew, T. Gruendl, G. Boehm, R. Meyer, and M.-C. Amann, IEEE J. Sel. Top. Quantum Electron. **19**(4), 1900909–1900917 (2013).
[18]R. Wang, S. Sprengel, G. Boehm, M. Muneeb, R. Baets, M. C. Amann, and G. Roelkens, Opt. Express **24**(18), 21081–21089 (2016).
[19]S. Keyvaninia, M. Muneeb, S. Stankovic, P. J. V. Veldhoven, D. V. Thourhout, and G. Roelkens, Opt. Mater. Express **3**(1), 35–46 (2013).
[20]G. Morthier and P. Vankwikelberge, *Handbook of Distributed Feedback Laser Diodes* (Artech House, Boston, MA, 1997).

Reuse of AIP Publishing content is subject to the terms at: https://publishing.aip.org/authors/rights-and-permissions. Download to IP: 157.193.240.1 On: Fri, 02 Dec 2016 14:22:46